Biochimica et Biophysica Acta 1818 (2012) 679–688

Contents lists available at SciVerse ScienceDirect

Biochimica et Biophysica Acta

journal homepage: www.elsevier.com/locate/bbamem

Heterologous production and characterisation of two distinct dihaem-containing membrane integral cytochrome b_{561} enzymes from *Arabidopsis thaliana* in *Pichia pastoris* and *Escherichia coli* cells

Lucia Cenacchi [a,1,2], Manuela Busch [b,1], Philipp G. Schleidt [a,b], Florian G. Müller [a,b], Tina V.M. Stumpp [a,3], Werner Mäntele [c], Paolo Trost [d], C. Roy D. Lancaster [a,b,*]

[a] Max Planck Institute of Biophysics, Department of Molecular Membrane Biology, Max von Laue Str. 3 D-60438 Frankfurt (Main), Germany
[b] Saarland University, Department of Structural Biology, Institute of Biophysics, Human and Molecular Biology Center, Faculty of Medicine, Building 60, D-66421 Homburg (Saar), Germany
[c] Goethe University, Institute of Biophysics, Max von Laue-Straße 1, D-60438 Frankfurt, Germany
[d] University of Bologna, Laboratory of Molecular Plant Physiology, Department of Biology, Via Irnerio 42, I-40126 Bologna, Italy

ARTICLE INFO

Article history:
Received 11 February 2011
Received in revised form 29 October 2011
Accepted 31 October 2011
Available online 7 November 2011

Keywords:
Arabidopsis thaliana
Biochemical characterisation
Cytochrome b_{561} paralog
Heterologous production
Membrane protein

ABSTRACT

Cytochrome (cyt) b_{561} proteins are dihaem-containing membrane proteins, belonging to the CYBASC (cytochrome-b_{561}-ascorbate-reducible) family, and are proposed to be involved in ascorbate recycling and/or the facilitation of iron absorption. Here, we present the heterologous production of two cyt b_{561} paralogs from *Arabidopsis thaliana* (*Acytb*$_{561}$-A, *Acytb*$_{561}$-B) in *Escherichia coli* and *Pichia pastoris*, their purification, and initial characterisation. Spectra indicated that *Acytb*$_{561}$-A resembles the best characterised member of the CYBASC family, the cytochrome b_{561} from adrenomedullary chromaffin vesicles, and that *Acytb*$_{561}$-B is atypical compared to other CYBASC proteins. Haem oxidation–reduction midpoint potential (E_M) values were found to be fully consistent with ascorbate oxidation activities and Fe^{3+}-chelates reductase activities. The ascorbate dependent reduction and protein stability of both paralogs were found to be sensitive to alkaline pH values as reported for the cytochrome b_{561} from chromaffin vesicles. For both paralogs, ascorbate-dependent reduction was inhibited and the low-potential haem E_M values were affected significantly by incubation with diethyl pyrocarbonate (DEPC) in the absence of ascorbate. Modification with DEPC in the presence of ascorbate left the haem E_M values unaltered compared to the unmodified proteins. However, ascorbate reduction was inhibited. We concluded that the ascorbate-binding site is located near the low-potential haem with the Fe^{3+}-chelates reduction-site close to the high-potential haem. Furthermore, inhibition of ascorbate oxidation by DEPC treatment occurs not only by lowering the haem E_M values but also by an additional modification affecting ascorbate binding and/or electron transfer. Analytical gel filtration experiments suggest that both cyt b_{561} paralogs exist as homodimers.

1. Introduction

Cytochrome (cyt) b_{561} proteins are di-haem containing membrane proteins that can shuttle one electron across the lipid bilayer and belong to the eukaryotic redox protein family CYBASC [1,2]. The function of the CYBASC proteins has mostly been correlated with ascorbate recycling [3–7] and/or facilitation of iron absorption [8–12]. In animals and plants, several CYBASC paralogs were shown to be present [1]. Multiple alignment of amino acid sequences of various CYBASC members has suggested that they all possess a conserved three-dimensional (3-D)

Abbreviations: A_x, absorption at a wavelength of x nm; BCA, bicinchoninic acid; BMGY, buffered glycerol-complex medium; BMMY, buffered methanol-complex medium; BSA, bovine serum albumin; CV, column volumes; CYBASC, cytochrome b_{561} ascorbate reducible family; cyt b_{561}, cytochrome b_{561}; Da, Dalton; $\Delta E_{M,bH}$, shift in $E_{M,bH}$; $\Delta E_{M,bL}$, shift in $E_{M,bL}$; DEPC, diethyl pyrocarbonate; DDM, n-dodecyl-β-D-maltoside; DMSO, Dimethyl sulfoxide; DTT, Dithiothreitol E_M, oxidation–reduction midpoint potential; $E_{M7.2}$, E_M value at pH 7.2; $E_{M,bH}$, E_M of the high-potential haem; $E_{M,bL}$, E_M of the low-potential haem; ESI, Electrospray ionisation; FOS-12, Fos-choline 12, $H_{10,}$ deca-histidine affinity tag; IEF, isoelectric focusing; IMAC, immobilised metal affinity chromatography; IPTG, Isopropyl β-D-1-thiogalactopyranoside; LB, Luria-Bertani; MDHA, mono-dehydroascorbate; MNNG, N-methyl-N′-nitro-N-nitrosoguanidine; MS, Mass spectrometry; MW, molecular weight; M9, Salts Minimal Media; NZYM, NZ amine; NaCl, bacto-yeast extract and magnesium sulphate; OD_x, optical density at a wavelength of x nm; ORF, open reading frame; RCA, relative catalytic activity; S_{II}, streptavidin affinity tag II; *S. c.*, *Saccharomyces cerevisiae*; SDS-PAGE, sodium dodecyl sulphate polyacrylamide gel electrophoresis; TMPD, N,N,N′,N′,tetramethyl-p-phenylenediamine dihydrochloride; YNB, Yeast Nitrogen Bases; *Zm*, *Zea mays*

* Corresponding author at: Saarland University, Department of Structural Biology, Institute of Biophysics, Human and Molecular Biology Center, Faculty of Medicine, Building 60, D-66421 Homburg (Saar), Germany. Tel.: +49 6841 16 26235; fax +49 6841 16 26251.
E-mail address: Roy.Lancaster@structural-biology.eu (C.R.D. Lancaster).
[1] These authors contributed equally.
[2] Present address: COC Farmaceutici s.r.l., Via Modena 15, I-40019 Sant'Agata Bolognese (BO), Italy.
[3] Present address: Labor Prof. Enders & Partner, Abteilung Molekulargenetik/Pharmakogenetik, Rosenbergstraße 85, D-70193 Stuttgart, Germany.

0005-2736/$ – see front matter © 2011 Elsevier B.V. All rights reserved.
doi:10.1016/j.bbamem.2011.10.030

structure with six highly hydrophobic areas predicted to form membrane-spanning α-helices, four conserved His residues likely to be involved in the coordination of two haem *b* centres, and the putative ascorbate and mono-dehydroascorbate (MDHA) binding motifs [1,13–15] (Supplementary Fig. S1). While investigation of animal CYBASC members has proceeded rapidly in the recent years, little has been presented on plant CYBASC and the physiological function in plants of this redox family is still unknown. The first putative cyt b_{561} purified from the plasma membrane of bean hypocotyls (*P*cytb_{561}-I), was long believed to be the plant counterpart of the bovine chromaffin granule cyt b_{561} [16,17]. However, a recent extensive biochemical characterisation of *P*cytb_{561}-I has shown that this cytochrome is not a CYBASC member [18]. To date, the purified plant CYBASC proteins are the *A*cytb_{561}-A from *Arabidopsis thaliana* [8,19,20], *C*cytb_{561}-A from wild water melon [21], a cyt b_{561} from bean (*P*cytb_{561}-II) [22] and one protein from *Zea mays* (Zmcytb_{561}) [23]. Although all these proteins displayed typical CYBASC features, they have been found in different subcellular compartments and may perform different physiological functions. For instance, *A*cytb_{561}-A and the *P*cytb_{561}-II from bean are localised in the tonoplast and both are proposed to be involved in iron homeostasis [8,18,19], while the *C*cytb_{561}-A has been identified in the plasma membrane and is proposed to be involved in energy dissipation [21].

The *A. thaliana* genome appears to contain four cytb_{561} genes [1,24,25]. Based on microarray data and ESTs (expressed sequence tags), all of them are expressed in vivo (RNA level). On the protein level, the two genes *artb561-a* and *artb561-b* were shown to be expressed [13,19,26]. In addition, expression of cytb_{561} proteins was shown in *Rhaphanus sativus* [26].

Currently, no experimentally determined three-dimensional atomic model of any CYBASC member has been reported. Therefore, studies that enable production of CYBASC members are essential to future structural studies of representatives of this superfamily. Here we present the heterologous production in *Escherichia coli* and *Pichia pastoris* strains and the initial biochemical characterisation of *A*cytb_{561}-A and *A*cytb_{561}-B, two distinct members of the CYBASC family. The absorbance spectra of reduced *A*cytb_{561}-B differed from those of chromaffin granule cyt b_{561} and *A*cytb_{561}-A. However, biochemical characterisation of the purified *A*cytb_{561}-A and *A*cytb_{561}-B confirmed that both proteins are CYBASC members.

2. Material and methods

2.1. Generation of expression constructs

In order to introduce the coding sequence for the streptavidin affinity tag II (S_{II}) and deca-histidine (H_{10}) affinity tag into the pPIC3.K expression vector (Invitrogen), two complementary ssDNA oligonucleotides were synthesised (around 90 base pairs each), annealed and ligated to the pPIC3.5K plasmid previously digested with *Bam*HI/*Not*I restriction endonucleases (BioLab). The *artb561-b* ORF was amplified by PCR using the ′CGG AAT TCG CGG TTC CGG TGC TG′ and′CGA CCC TAG GTT GTG TGA GAA CTT GAT CC′ primers. Fragments were digested with the *Avr*II and *Eco*RI restriction endonucleases (BioLab) and cloned into the *Avr*II and *Eco*RI restriction sites of the pPIC3.5K-S_{II}/H_{10} derivative. In order to insert the ORFs encoding for the cyt b_{561} proteins into the pBAD expression vector derivatives, *artb561-a* was amplified using the ′GTA GCT GAG ATC TTC GCT GTC CGG ATA AAC′ and ′GTA GCT GGA ATT CGC TAT AGC AGA ATA ACT′ primers while the *artb561-b* was amplified with ′GTA GCT GAG ATC TTC GCG GTT CCG GTG CTG′ and ′GTA GCT GGA ATT CCG TTG TGT GAG AAC TTG′ primers. The DNA fragments so obtained and the pBAD expression vector derivatives were digested with *Bgl*II and *Eco*RI restriction endonucleases (BioLab) and ligated together. In all cases, the correct insertion of the ORFs into the expression vector derivatives was verified by colony PCR, restriction analysis and DNA sequencing (SeqLab GmbH, Göttingen).

2.2. Protein production in P. pastoris and membrane preparation

Protein production in *P. pastoris* was performed essentially as described previously for other membrane proteins by Weiss and coworkers [27] and is described in detail in the supplementary material. Normally from 12 L of cell culture, 100–120 g wet weight of cell pellet were obtained. The membrane preparation steps are described in detail in the supplementary material.

2.3. Creation of a methionine-auxotrophic E. coli strain

Methionine-auxotrophic strains of *E. coli* Top10-pRARE (F- *mcr*A Δ(*mrr-hsd*RMS-*mcr*BC) φ80*lac*ZΔM15 Δ*lac*X74 *rec*A1 *ara*D139 Δ(*araleu*) 7697 *gal*U *gal*K *rps*L (StrR) *end*A1 *nup*G) (Invitrogen) were obtained after mutagenesis with N-methyl-N′-nitro-N-nitrosoguanidine (MNNG) and negative selection using ampicillin [28]. The procedure is described in detail in the supplementary material.

2.4. Protein production in E. coli and membrane preparation

Protein production in *E. coli* was performed essentially as described previously for other membrane proteins by Surade and coworkers [29] and is described in detail in the supplementary material. Normally from 24 L cell culture, 40–60 g wet weight of cell pellet were obtained. The membrane preparation steps are described in detail in the supplementary material.

2.5. Protein quantification and purification (by IMAC)

Protein concentration was determined using the BCA Kit (Pierce) protocol [30] using bovine serum albumin (BSA) as a standard. Purified proteins were concentrated by pressure dialysis using 14 mL concentrators with a cut-off of 30 kDa (Amicon). Purification was performed using cell membranes obtained from, respectively, 2 L of *P. pastoris* or 24 L of *E. coli* cell culture. All chromatographic steps were performed at 4 °C with ice-cold buffers and at a flow rate of 0.5 ml/min on an ÄKTA Purifier system (GE Healthcare). Cell membranes at 5 mg/mL total protein concentration were solubilised in the dark with constant stirring at 4 °C for 2 h in 50 mM Na-phosphate pH 7.2, 350 mM NaCl, 10% glycerol (buffer A), with the addition of 1% Fos-choline 12 (Fos12), 25 mM ascorbate, 1 M betaine and 0.5 mM histidine. Insoluble material was separated from solubilised proteins by ultracentrifugation at 100,000 × *g* for 1 h at 4 °C. The supernatant was filtered through a 0.2 μm filter and loaded onto a HisTrap™ column (GE Healthcare) pre-equilibrated in 50 mM Na-phosphate pH 7.2, 350 mM NaCl, 10% glycerol, 0.1% Fos12 (buffer A1). The column was washed with 10 column volumes (CV) of buffer A1. In order to exchange the detergent from Fos12 to n-dodecyl-β-D-maltoside (DDM), the column was equilibrated with 5 CV of buffer A2 (50 mM Na-phosphate pH 7.2, 350 mM NaCl, 10% glycerol, 0.1% DDM). This was followed by a second wash in buffer A2 mixed with 2.5% buffer B (50 mM Na-phosphate pH 7.2, 350 mM NaCl, 10% glycerol, 250 mM histidine, 15 mM ascorbate, 5 mM betaine). The recombinant cyt b_{561} was eluted from the column in 100% buffer B.

2.6. Analytical gel filtration

The IMAC-purified cyt b_{561} proteins were analysed using a Superdex 200 PV 3.2/30 gel filtration column on a Smart chromatographic station (GE Healthcare). The Superdex 200 column was equilibrated at room temperature with at least 2.5 bed volumes of buffer A2 (50 mM Na-phosphate pH 7.2, 350 mM NaCl, 10% glycerol, 0.1% DDM). 50 μL of 1 mg/ml purified recombinant cyt b_{561} proteins were loaded onto the Superdex 200 column at 40 μL/min flow rate and aliquots of 60 μL each were collected during the separation. Both sample absorbance at 280 nm (A_{280}) and at 415 nm (A_{415}) were monitored continuously. Aliquots corresponding to the peak of the A_{280} and/or A_{415} were analysed by electrophoresis on SDS-polyacrylamide gels.

2.7. Photometric haem quantification

Absorption spectra were recorded by means of a double beam Lambda 40 model spectrophotometer (PerkinElmer) at room temperature. The amount of purified cyt b_{561} was estimated based on the haem content that was calculated by subtracting the absorbance at 575 nm (A_{575}) from the absorbance at 561 nm (A_{561}), divided by the molar absorption coefficient of 34.2 $mM^{-1}\,cm^{-1}$ [31], divided by two in a reduced (dithionite-treated) minus oxidised (ferricyanide-treated) spectra.

2.8. Modification with DEPC

The recombinant purified *A*cyt*b*$_{561}$ proteins (2–5 μM) were oxidised completely with final concentrations of 400 μM ferricyanide, as monitored spectrophotometrically between 400 nm and 600 nm. To remove the ferricyanide, the samples were passed through a PD10 desalting column (GE Healthcare) and re-equilibrated in buffer A2 (50 mM Na-phosphate pH 7.2, 350 mM NaCl, 10% glycerol, 0.1% DDM) and another spectrum between 400 and 600 nm was recorded. The oxidised sample was then divided into aliquots and diluted with equal volume of, respectively, buffer A2 (negative control), 10 mM DEPC in buffer A2, and 10 mM DEPC with 25 mM ascorbate in buffer A2. After incubation at room temperature for 1 h in the dark, all samples were re-equilibrated in buffer A2 using a PD10 column and concentrated to 1 μM. Absorption spectra were recorded before and after addition of 5 mM ascorbate and after the addition of solid dithionite.

2.9. Reduction of ferric chelates

To stably reduce the cytochromes, the recombinant purified *A*cyt*b*$_{561}$ proteins (2 μM) were incubated for 15 min at room temperature in the dark with 40 mM ascorbate and 10 mM betaine in buffer A (50 mM Na-phosphate pH 7.2, 10% glycerol, 350 mM NaCl, 0.1% DDM). Ascorbate and betaine removal was achieved by re-equilibration in buffer A using a PD10 column. Spectra were recorded before and after the addition of 4 mM, 8 mM and 16 mM Fe^{3+}-EDTA. The procedure was analogous for Fe^{3+}-citrate. For the kinetic activity measurements, the paralogs were incubated with 100 mM ascorbate over night, after which ascorbate was removed using a PD10 column. Measurements were started by adding 2 μM of the Fe^{3+} chelates. The activities were calculated from the time dependence of the $A_{561} - A_{575}$ absorption differences. One unit (U) is defined as the amount of cytochrome b_{561} proteins which is oxidised by the Fe^{3+}-chelates (or which is reduced by ascorbate, see Section 2.12).

2.10. Determination of haem midpoint potentials of the recombinant purified Acytb$_{561}$ proteins

Using the electrochemical cell described earlier [32], haem oxidation–reduction midpoint potentials of purified *A*cyt*b*$_{561}$-A and *A*cyt*b*$_{561}$-B were determined by potentiometric titrations, in analogy to previously published procedures for other dihaem-containing membrane proteins [33–35] and described in detail in the supplementary material.

2.11. Isoelectric focusing of the recombinant purified Acytb$_{561}$ proteins

At least 0.5 mg of recombinant purified *A*cyt*b*$_{561}$ proteins were analysed in a pH range of 3 to 10 by liquid phase isoelectro focusing (IEF) using the Rotofor™Cell (BioRad) following the specifications of the manufacturer.

2.12. Kinetic analysis of ascorbate oxidation

The samples were treated as described in Section 2.8. Measurements were started by the addition of 5 μM ascorbate. Initial rates were determined by a linear fit to the time dependence of the $A_{561} - A_{575}$ absorption differences. In order to facilitate the discussion, the values obtained for the controls were set to be 100% and the catalytic activities determined for the different samples were expressed as relative catalytic activities (RCA).

3. Results

3.1. Heterologous production and purification of the Acytb$_{561}$ proteins in yeast and bacterial cells

The *artb561-a* and *artb561-b* ORFs, coding for two putative cyt b_{561} paralogs, were expressed in *P. pastoris* and in *E. coli* cells (see Supplementary Figs. S2 and S3). Based on the characterisation performed to date and apart from the production yield, there were no differences apparent between the two production systems. The recombinant proteins obtained were named according to the name of the paralog, with the expression system indicated in the superscript (^{Pp} for *P. pastoris* and ^{Ec} for *E. coli*) and the affinity tag associated with the recombinant cytochromes indicated in the subscript, e.g. the *A*cyt*b*$_{561}$-B produced in *P. pastoris* in frame with the S_{II} and H_{10} affinity tags was named ^{Pp}*A*cyt*b*$_{561}$-B_{SH} (Table 1).

We found that the respective induction times of 20 h for *P. pastoris*, of 3 h (B-paralog) and of 5 h (A-paralog) for *E. coli* were sufficient to obtain the maximum yield (see Material and methods). Immunoblot analysis against the His affinity tag of cell membranes obtained

Table 1
Recombinant cytochromes produced in *P. pastoris* and in *E. coli*.

Name of recombinant protein	Expression system strain	N-term fusion tag	paralog	C-term fusion tag	MW [1] (kDa)	Apparent MW (kDa) SDS-PAGE	Apparent MW (kDa) GF	Cal. pI[1]	Exp. pI
^{Ec}*A*cyt*b*$_{561}$-A_H	*E. coli* Top10 pRare met$^-$	No tag	cyt*b*$_{561}$-A	Tev, H_{10}	29.2	26	100	6.7	6.7
^{Ec}*A*cyt*b*$_{561}$-B_{HS}	*E. coli* C43$^-$	H_6, Tev	cyt*b*$_{561}$-B	S_{II}	29.6	24	137	9.1	n.d.
^{Pp}*A*cyt*b*$_{561}$-B_{SH}	*P. pastoris* SMD1163	S_{II}	cyt*b*$_{561}$-B	H_{10}	29.5	22	147	9.4	9.4

Abbreviations: meth$^-$, methionine auxotrophic; N-term, amino-terminus; C-term, carboxy-terminus; MW, molecular weight; cal, calculated; [1]data obtained using ExPaSy (http://www.expasy.ch/); Exp, experimental; SDS-PAGE, sodium dodecyl sulphate polyacrylamide gel electrophoresis; GF, gel filtration; pI, isoelectric point; TEV, coding sequence for tobacco etch virus (TEV) protease consensus sequence; H_6, hexa-histidine affinity tag; H_{10}, deca-histidine affinity tag; S_{II}, streptavidin affinity tag II.

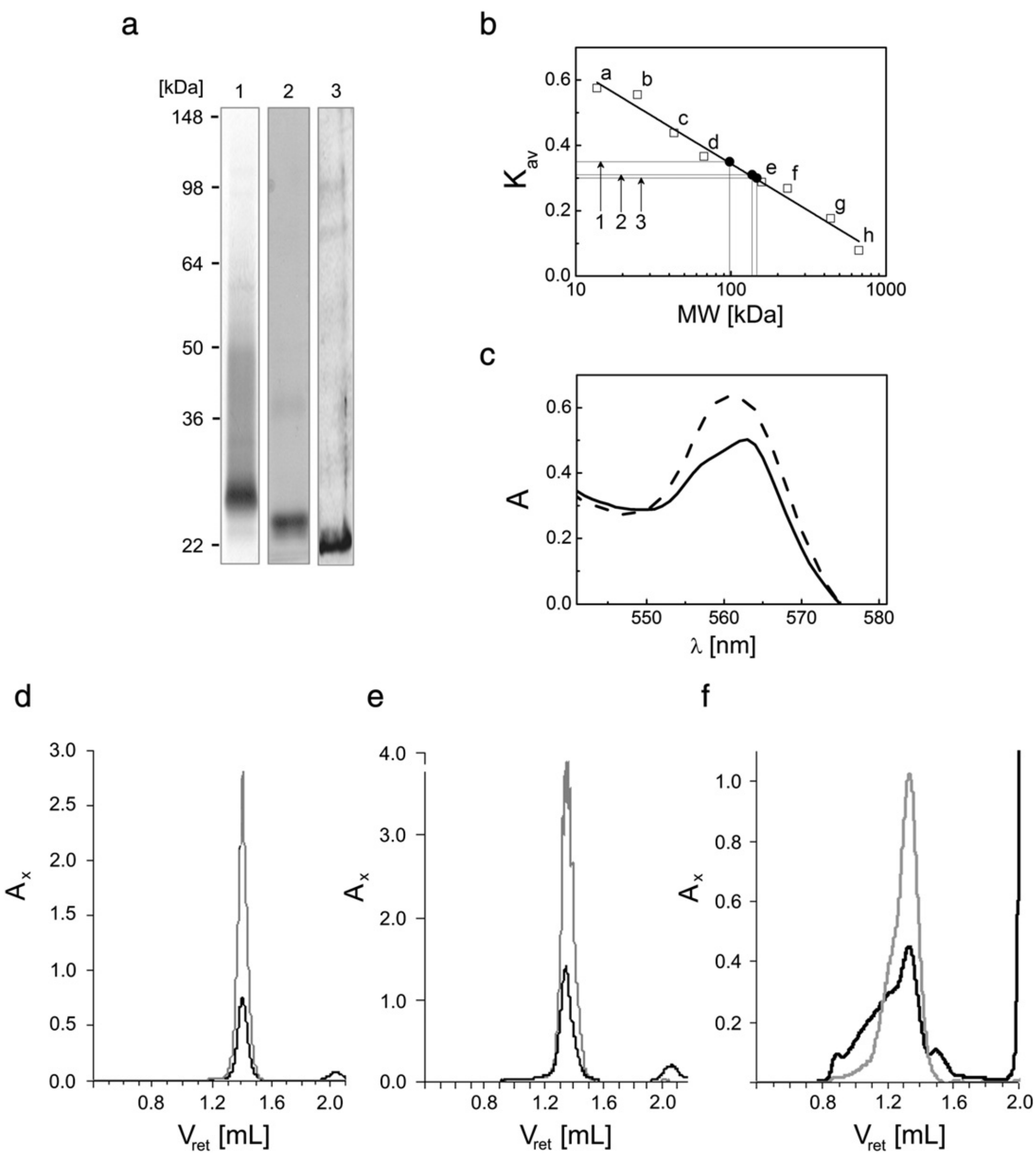

Fig. 1. SDS-PAGE and Western Blot, analytical gel filtration and oligomeric state analyses of the purified recombinant cyt b_{561} proteins from *A. thaliana*. (a) Fractions from the affinity column containing the purified cytochrome were pooled and purity assessed by SDS-PAGE analysis. Lane 1: purified ^{Ec}Acytb_{561}-A_H (SDS-PAGE); lane 2: purified ^{Ec}Acytb_{561}-B_{HS} (Western Blot); lane 3: purified ^{Pp}Acytb_{561}-B_{SH} (SDS-PAGE). (b) Molecular weight calibration using a Superdex 200 PV 3.2/30 gel filtration column on a Smart Chromatographic station (GE Healthcare). The eight proteins shown in the figure (and their molecular weights) are: ribonuclease A (a, 13.7 kDa), chymotrypsinogen (b, 25 kDa), ovalbumin (c, 43 kDa), albumin (d, 67 kDa), aldolase (e, 158), catalase (f, 232 kDa), ferritin (g, 440 kDa), and thyroglobulin, (h, 669 kDa). Using this MW calibration, the MW of the three protein-detergent complexes specified in panel a 1–3 were determined as listed in Table 1; K_{av}: partition coefficient [62]. (c) Comparison of the dithionite reduced minus ferricyanide oxidised visible-spectra of ^{Ec}Acytb_{561}-A_H (solid line, asymmetric maximum at 562 nm and a shoulder at 557 nm) and ^{Ec}Acytb_{561}-B_{HS} (dashed line, symmetric maximum at 561 nm). (d–f) Homogeneity analysis by size-exclusion chromatography using a Superdex 200 column (Pharmacia). The symbol x in A_x stands for 280 nm (black) and 415 nm (grey) (d) ^{Ec}Acytb_{561}-A_H, retention volume (V_{ret}) = 1.4 mL (e) ^{Ec}Acytb_{561}-B_{HS} (V_{ret} = 1.34 mL) and (f) ^{Pp}Acytb_{561}-B_{SH} (V_{ret} = 1.33 mL). The increase of absorbance at 280 nm at the end of the run of the analytical gel filtration was due to the presence of ascorbate (maximum absorbance at 340 nm). SDS-PAGE analysis of the corresponding fractions revealed no protein band (data not shown). In addition, when analytical gel filtration of ^{Ec}Acytb_{561}-A_H (d) and ^{Pp}Acytb_{561}-B_{SH} (e) was performed in the absence of ascorbate, this peak did not appear.

from transformed *P. pastoris* cells revealed the production of the ^{Pp}Acytb_{561}-B_{SH} as a single band of 22 kDa (Figs. 1a and S2). The same analysis of membranes from transformed *E. coli* cells revealed the presence of ^{Ec}Acytb_{561}-A_H as a single band at 26 kDa and of ^{Ec}Acytb_{561}-B_{HS} at 24 kDa (Figs. 1a and S3). In both the yeast and the bacterial expression systems, no band was detected in the immunoblot of the cell membranes of untransformed cells and of cells transformed with empty vector (data not shown).

Immunoblot analyses indicated that the highest solubilisation level of the recombinant cytochromes was obtained with the detergent Fos12 (Table 2). The recombinant cytochromes were purified by a single step immobilised metal affinity chromatography (IMAC) (Fig. 1a). During IMAC, the Fos12 detergent was replaced by the neutral detergent DDM. In order to preserve the amount of reducible haem of the purified paralogs, we added 15 mM ascorbate and 5 mM betaine to the elution buffer. The recombinant proteins purified following this strategy were pure (Fig. 1a), homogeneous (Fig. 1b, d–f), and stable (Fig. S5). Comparison of the retention volume observed from the analytical gel filtration of the purified Acytb_{561} proteins with the MW calibration generated (described in Fig. 1b) indicates that both cytochromes are present in the dimeric form when solubilised (Table 1). Similar results were also reported for the cyt b_{561} from bovine chromaffin vesicle produced in *P. pastoris* [31] and for the Pcytb_{561}-II [18].

Table 2
Purification of recombinant Acytb_{561} proteins heterologously produced in *E. coli* (24 L) and *P. pastoris* cells (2 L).

Production system	Paralog	Total protein (mg)	Total cyt b_{561} (mg)	Yield (%)	Purification fold
E. coli	^{Ec}Acytb_{561}-A_H				
	Fos12 extracted	750	3.6*	100	1
	IMAC purified	1.6	1#	28	130
E. coli	^{Ec}Acytb_{561}-B_{HS}				
	Fos12 extracted	600	4.0*	100	1
	IMAC purified	1.7	1.1#	28	96
P. pastoris	^{Pp}Acytb_{561}-B_{SH}				
	Fos12 extracted	1000	7.7	100	1
	IMAC purified	2	1#*	13	75

The specific content of cyt b_{561} was determined from the differences between ascorbate-reduced* or dithionite-reduced# against the ferricyanide-oxidised absorbance spectra as described in experimental procedures.

3.2. Electronic absorbance characteristics of purified recombinant Acytb_{561} proteins

The spectrum of the purified A-paralog displayed the typical asymmetric α-band (Fig. 1c), similar to the native and recombinant bovine chromaffin vesicle cyt b_{561} [36,37], whereas that of the B-paralog displayed a symmetric α-band with its maximum centred at 561 nm (Fig. 1c). This difference is not attributable to the use of different expression systems, as the reduced-minus-oxidised absorbance spectra of Acytb_{561}-B produced either in *P. pastoris* or in *E. coli* cells were virtually identical (see Supplementary Fig. S4). In addition, this feature is not due to the loss of any haem centre. Analysis of the cofactor content was found to be 1.7 haem groups per cyt b_{561} monomer both for the purified ^{Ec}Acytb_{561}-A_H and ^{Ec}Acytb_{561}-B_{HS}. This ratio is in the range reported for bovine chromaffin vesicle cyt b_{561} from native and heterologous sources [38]. The presence of two titratable haem centres was also confirmed by potentiometric titrations monitoring the α-band absorbance. The values of the haem oxidation–reduction midpoint potentials of the purified Acytb_{561} proteins (Fig. 2a and b) were in the same range as those of animal chromaffin vesicle cyt b_{561} [39–41]. Furthermore we could confirm independently the haem redox midpoint potentials for the A-paralog which were published by Desmet et al. in 2011 [20].

Consistent with the haem redox midpoint potentials of the two paralogs, both cytochromes were promptly reduced by ascorbate. This compound is believed to be the physiological electron donor of cyt b_{561} proteins [13,18]. Therefore, the reduction by ascorbate of both purified cytochromes was monitored and relative catalytic activities were calculated (Fig. 2c and d). Even at high ascorbate concentrations (40 mM), full reduction of both haem centres was not achievable. This could, however, be observed when using the non-physiological reductant sodium dithionite. The ascorbate reducibility of *A. thaliana* paralogs resembled that of *P*cytb_{561}-II [18]. All plant CYBASC proteins studied (*P*cytb_{561}-II and both *A. thaliana* paralogs in this work) could be reduced only up to 80% by ascorbate (Fig. 3e and [18]).

In addition we found that both paralogs could be oxidised by different Fe^{3+} chelates (Fe^{3+}-EDTA and Fe^{3+}-citrate, Fig. 3a–d) [8,18,19]. Since the ferric-reductase activity of the non inhibited A-paralog was too high for kinetic measurements in our experimental setup, we used the DEPC modified A-paralog in its place. In contrast to the A-paralog the activities of B-paralog could be measured without any inhibition (Fig. 3f). Our results indicated that the reduction of Fe^{3+} -EDTA is higher than that of Fe^{3+} -citrate. We found the specific activity for the reduction of Fe^{3+} EDTA to be 1.2 U/mg (+/−0.4 U/mg) for the modified A-paralog and 0.6-U/mg (+/−0.1 U/mg) for the B-paralog (Fig. 3f). For the reduction of Fe^{3+}-citrates, the specific activities were 0.05 U/mg (+/−0.0005; A-paralog) and 0.14 U/mg (+/−0.04; B-paralog).

3.3. Effect of pH on the ascorbate-dependent reduction and stability of the recombinant Acytb_{561} proteins

The experimental pI values of the purified ^{Ec}Acytb$_{561}$-A_H and ^{Pp}Acytb_{561}-B_{SH} were investigated by analytical liquid-phase IEF (BioRad) with the pH value of the electrolyte ranging 3 to 10. All fractions were analysed by SDS-PAGE and the amount of the dithionite reducible haem was calculated as previously described (see Supplementary Fig. S6). The results revealed that the A-paralog was clearly more acidic (pI = 6.7) than the B-paralog (pI = 9.2) (Table 1). The deduced pI values for other animal and plant CYBASC proteins are generally in the same range; e.g. the pI value of bovine chromaffin granule cyt b_{561} is 6.2 [41], the calculated pI values of human duodenal cyt b_{561} is 9.12 and that of human lysosomal cyt b_{561} is 9.48. All theoretical pI data were calculated using the ProtParam tool software (http://www.expasy.ch/tools/protparam.html, [42]). The observed pI values of the purified *A. thaliana* cyt b_{561} paralogs were surprisingly

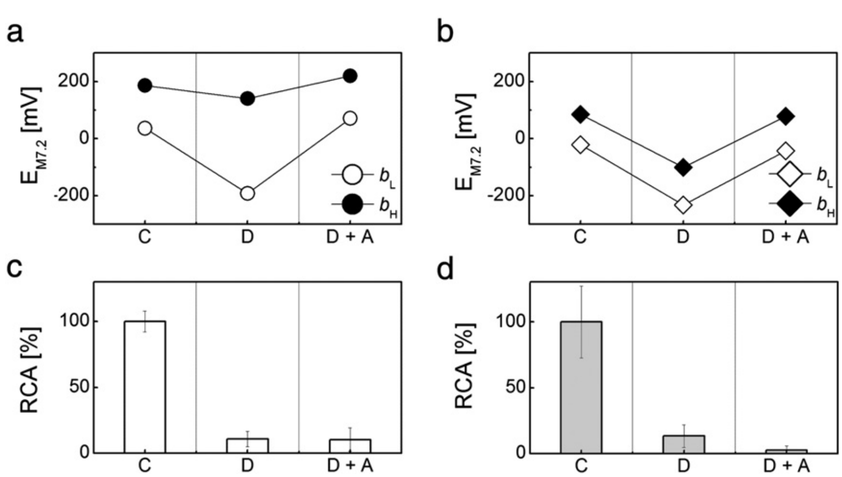

Fig. 2. Overview of the values of the redox midpoint potential of the haem *b* groups and of the relative catalytic activities (RCA) of the A- and B-paralog. Purified cytochromes samples were portioned and the samples were not treated (C), treated with DEPC (D) or with DEPC and ascorbate (D + A). Haem-potentiometric reductive-oxidative titrations of the different samples (C, D, D + A) were performed with the electrochemical cell [32]. Comparison of the different $E_{M7.2}$ values of the A- paralog (a) and of the B-paralog (b). For the kinetic activity measurements of ascorbate oxidation, cytochrome samples were oxidised with ferricyanide. After ferricyanide removal, the kinetic measurements were started by adding 5 μM ascorbate. (c, d) Relative catalytic activities of the A-paralog (c) and B-paralog (d). The values of the controls were 2.2 U/mg (+/−0.2 U/mg; A-paralog) and 12.8 U/mg (+/−3.5 U/mg; B-paralog).

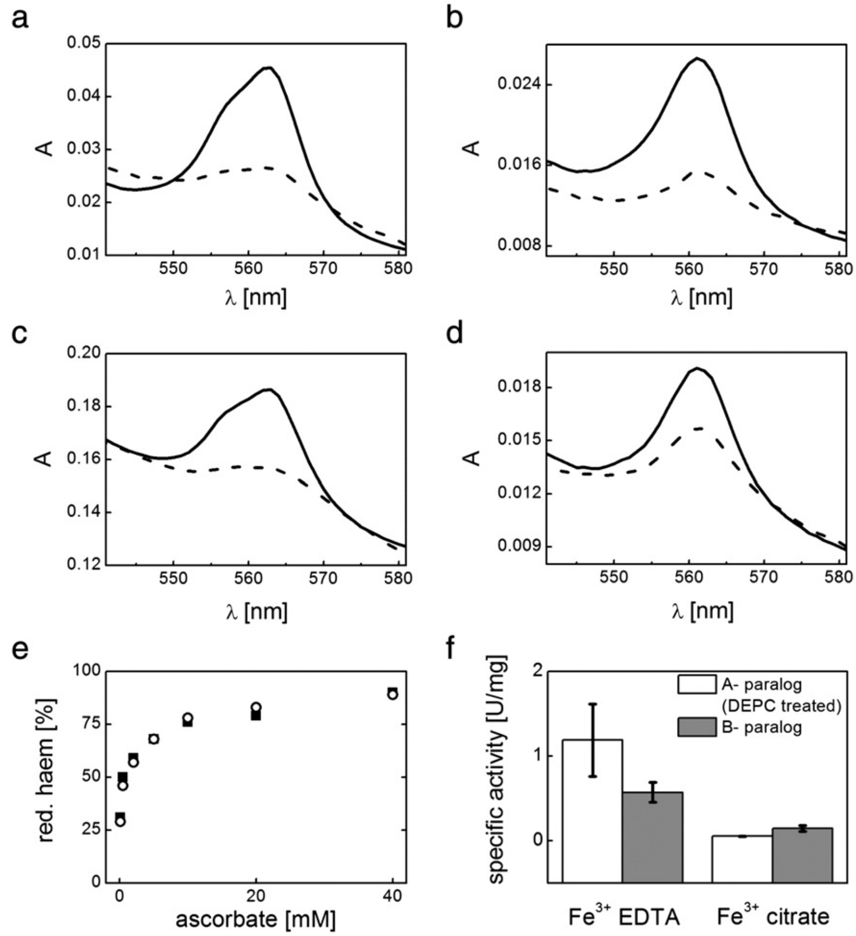

Fig. 3. Biochemical characterisation of purified ^{Ec}Acytb_{561}-A$_H$ and ^{Pp}Acytb_{561}-B$_{SH}$ via absorbance spectroscopy. Ferric-reductase activity of the purified cytochromes was evaluated after reduction with 40 mM ascorbate (black lines in panels a, b, c and d). Prior to the addition of the Fe^{3+}-chelate, samples were equilibrated in the same buffer without reductants and a new spectrum was recorded. Oxidation of the (a) ^{Ec}Acytb_{561}-A$_H$ by Fe^{3+}-EDTA (dashes), (b) ^{Pp}Acytb_{561}-B$_{SH}$ by Fe^{3+}-EDTA (dashes), (c) ^{Ec}Acytb_{561}-A$_H$ by Fe^{3+}-citrate (dashes), and (d) ^{Pp}Acytb_{561}-B$_{SH}$ by Fe^{3+}-citrate (dashes). (e) Reducibility at increasing concentrations of ascorbate of the purified ^{Ec}Acytb_{561}-A$_H$ (squares) and ^{Pp}Acytb_{561}-B$_{SH}$ (circle). Cytochromes were oxidised with 400 μM ferricyanide and then equilibrated in the same buffer without ferricyanide. 0.1 mM, 0.5 mM, 2 mM, 5 mM, 10 mM, 20 mM and 40 mM final concentration ascorbate were added directly to the cuvette. The percentages of the amount of ascorbate reduced haem were calculated with the respect to the amount of dithionite reducible haem. (f) Specific activities of ferric-chelate reduction of the DEPC-modified A-paralog and the untreated B-paralog. Samples were incubated with 100 mM ascorbate overnight, separated and the reaction was started by adding 2 μM Fe^{3+}-chelates. The changes in the A_{561} and A_{575} absorptions were monitored over the time.

similar to the predicted ones (Table 1). After the liquid-phase IEF experiments, the content of ascorbate- and dithionite-reducible haem in each fraction was determined (Fig. 4). Ascorbate reduction of the ^{Ec}Acytb$_{561}$-A$_H$ was increased at pH values lower than 6.5 (the difference between the reducibility obtained with ascorbate and dithionite is minimal), while already at pH values greater than 7.5, the ascorbate reduction was decreased (Fig. 4a). This decrease was less pronounced in the case of ^{Pp}Acytb_{561}-B$_{SH}$ (Fig. 4b). The sensitivity to mildly alkaline pH values of the two *Acytb*$_{561}$ proteins differed from the behaviour of the bovine chromaffin granule cyt b_{561} produced in bacterial cells that was reported to be unaffected by the change in pH [38]. In contrast, the native chromaffin granule cyt b_{561} was reported to be sensitive to alkaline pH [43–45]. For both purified *A. thaliana* cyt b_{561} proteins, the total haem reducibility (dithionite reducibility, Fig. 4a–b) showed a trend similar to that of the ascorbate reducibility. The decrease due to alkaline pH values was even more evident for the haem reducibility after two days of incubation at different pH values (Fig. 4c).

3.4. Inhibition by DEPC and redox titration of DEPC-modified recombinant Acytb$_{561}$ proteins

To ascertain whether the ascorbate-dependent reduction of A- and B-paralogs was inhibited by DEPC, samples oxidised previously with ferricyanide were incubated with DEPC either in the absence of ascorbate (sample "D" in Fig. 2) or in the presence of ascorbate (sample "D + A") and compared with unmodified samples (sample "C", control). After incubation, DEPC was removed from the sample and the haem reducibility of the modified samples was calculated by reduced-minus-oxidised spectra. Control *Acytb*$_{561}$ proteins were reducible by ascorbate and dithionite (Table 3 and Supplementary Fig. S7) and the haem content values calculated after addition of ascorbate or dithionite were respectively taken as 100% of the reduction achievable (Table 3). When the A-paralog was modified with DEPC, only 8% of the ascorbate-dependent reduction was achieved compared to the ascorbate-reduced control. Using dithionite, less than 73% of the haem reduction was obtained compared to the sodium dithionite-reduced ^{Ec}Acytb$_{561}$-A$_H$ control (Table 3). When incubation with DEPC was performed in the presence of ascorbate, the ascorbate dependent reduction was partially inhibited (42%) and the dithionite reduction was almost identical to the control (Table 3). A very similar scenario was observed for the B-paralog. When the B-paralog was modified with DEPC, only 36% of the ascorbate reduction compared to the control was achieved (Table 3). In contrast to the A-paralog, the DEPC modified B-paralog could be fully reduced by dithionite (112%). After incubation with DEPC in the presence of ascorbate, the ascorbate-dependent reduction was only partially inhibited (54%). Using dithionite, the B-paralog was reduced to an identical degree compared to the control (95%).

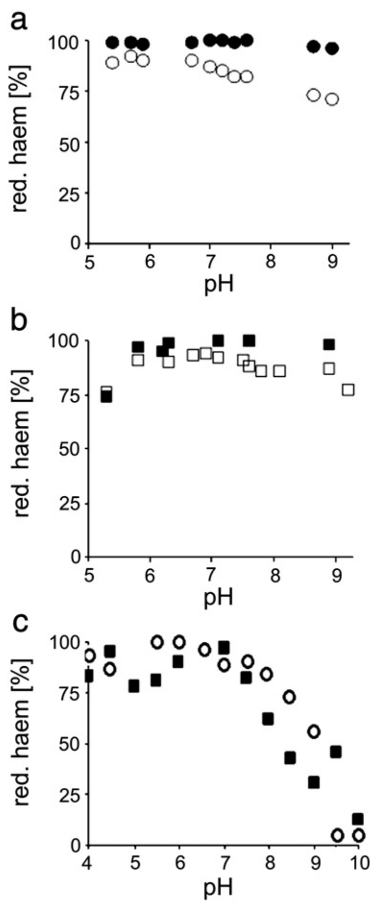

Fig. 4. Dependence on pH of ascorbate reducibility and of haem content for the recombinant *A. thaliana* cyt b_{561} paralogs. The purified cytochromes were separated by IEF. Haem groups reduction by ascorbate and dithionite of the fractions at different pH values were determined via spectroscopy. (a) Ascorbate reducibility (open circles) and dithionite reducibility (full circles) of ^{Ec}Acytb_{561}-A$_H$. (b) Ascorbate reducibility (open squares) and dithionite reducibility (full squares) of ^{Pp}Acytb_{561}-B$_{SH}$. (c) The amount of dithionite-reducible haem of ^{Ec}Acytb_{561}-A$_H$ (open circles) and ^{Pp}Acytb_{561}-B$_{SH}$ (full squares) was redeterminated after 2 days at room temperature and is shown as the percentage of the initial one (dithionite reduction of ^{Ec}Acytb_{561}-A$_H$ and ^{Pp}Acytb_{561}-B$_{SH}$ in panels a and b).

We also found an inhibition of the kinetic activities of the differently treated samples: The specific activities of the controls were set to be 100%. In comparison to the control (unmodified samples) the DEPC-modified A-paralog displayed a relative catalytic activity (RCA) of 11% and the DEPC-plus-ascorbate modified A-paralog of only 10%. For the B-paralog we monitored roughly the same effects: The DEPC-modified sample exhibited a RCA of 13% and the DEPC-plus-ascobate modified sample of only 3% (Fig. 2c and d). Ascorbate reduction of the Acytb_{561} proteins modified by DEPC in the absence (i) or presence (ii) of ascorbate was slower than that of the unmodified samples. These results matched the observations for cyt b_{561} from bovine chromaffin vesicles: It was reported that treatment with DEPC plus ascorbate led to a slower reduction of the high potential haem of the cyt b_{561} from bovine chromaffin vesicles [46–49].

To determine whether DEPC modified the haem midpoint potential, redox titrations were performed. The $E_{M7.2}$ values of the DEPC-modified Acytb_{561} proteins were analysed according to the same procedure used to analyse the unmodified ones. The redox titration curves confirmed the presence of two titratable haem centres (Supplementary Fig. S8). The values of the haem redox midpoint potential of the DEPC-modified-paralog were found to be −193 mV and 140 mV (before incubation with DEPC they were 36 mV and 187 mV), while the $E_{M7.2}$ values of B-paralog were found to be −233 mV and −101 mV (before incubation with DEPC they were −22 mV and 85 mV; Table 3 and Supplementary Fig. S8). The values of the haem redox midpoint potential of the DEPC-modified *A. thaliana* cyt b_{561} paralogs trigger new questions on the differences residing in both haem centres of the two paralogs. We thus performed new redox titrations with enzymes modified with DEPC and ascorbate. We found the haem redox midpoint potential values of the A-paralog modified with DEPC in the presence of ascorbate to be 71 mV and 220 mV, respectively. The values for the B-paralog after the same treatment were found to be −43 mV and 78 mV. These are displayed graphically for a better comparison in Fig. 2a and b.

4. Discussion

4.1. Production of Acytb_{561} paralogs for biochemical studies

Investigations of both cytochromes are of particular interest as no three-dimensional structure of any CYBASC member has been

Table 3
Overview of the specific midpoint potentials, dithionite and ascorbate haem reducibility of the recombinant Acytochrome b_{561} enzymes.

Reference	Enzyme	Substrate/ inhibitor	$E_{M,bL}$ [mV][a]	$E_{M,bH}$ [mV][a]	r[b]	Haem reducibility	
						asc[c]	di[d]
Desmet et al., 2007 [20]	$^{S.c.}$ Tcyt b_{561}	–	20 (+/−14)	178 (+/−15)			
This work	Cyt b_{561}- A	–	36 (+/−4)	187 (+/−2)	0.9917	100%[e]	100%[f]
This work	Cyt b_{561}- A	+ DEPC	−193 (+/−5)	140 (+/−4)	0.9614	8%[e]	73%[f]
This work	Cyt b_{561}- A	+ DEPC + ASC	71 (+/−6)	220 (+/−8.0)	0.9654	42%[e]	108%[f]
This work	Cyt b_{561}- B	–	−22 (+/−6)	85 (+/−3)	0.9940	100%[e]	100%[f]
This work	Cyt b_{561}- B	+ DEPC	−233 (+/−6)	−101 (+/−3)	0.9958	36%[e]	112%[f]
This work	Cytb_{561}- B	+ DEPC + ASC	−43 (+/−3)	78 (+/−2)	0.9828	54%[e]	95%[f]

[a] The standard deviations are shown in parentheses.
[b] r = correlation coefficient.
[c] asc = with ascorbate.
[d] di = with sodium dithionite.
[e] The haem reducibility by ascorbate of the not-treated sample is set to 100%. The values of the treated samples are relative to the not-treated sample.
[f] The haem reducibility by dithionite of the not-treated sample is set to 100%. The values of the treated samples are relative to the not-treated sample.

presented to date. In addition, only a few members of this family have been characterised biochemically and they are all related to the first identified CYBASC proteins, the bovine chromaffin vesicle cyt b_{561} or to the cytb_{561}-A from *A. thaliana*. These two members were characterised by the presence of an asymmetrical α-band in their absorption spectra, so that this asymmetry was regarded as a common feature of cyt b_{561} orthologs [18]. The heterologous production in *E. coli* and *P. pastoris* of a CYBASC protein described here that did not show this common spectroscopic feature, but conserved surprisingly well the other relevant biochemical characteristics, is thus of great importance. The symmetric α-band of *A*cytb_{561}-B demonstrated here excludes the asymmetry of the α-band as a common CYBASC feature. Apart from the description of cyt b_{561} from duodenum (*D*cytb$_{561}$ [9,11]), other CYBASC members, such as the lysosomal [7,50] and erythrocyte [12] cytb_{561} proteins, have so far not been characterised extensively. Therefore, the investigation of the *A*cytb_{561} enzymes may also facilitate a deeper understanding and biochemical investigations on these members. The identification of a CYBASC member that shows 'atypical' features has increased interest in this hydrophobic electron-transporter superfamily.

4.2. The dataset of the haem redox midpoint potentials is fully consistent with ascorbate oxidation activity and the Fe^{3+}-chelates reductase activity determined in this work

Due to the use of an accurate haem redox titration procedure (see Section 2.10 and the supplementary material), we present the first set of data that shows complete consistency between haem redox titration, ascorbate titration, the presence of the Fe^{3+}-chelates reductase activity and kinetic measurements for CYBASC members. Purified paralogs could not be reduced fully by ascorbate (up to 80% haem reduction even in the presence of 40 mM ascorbate, Fig. 2e) and full haem reduction was achieved only with dithionite. Accordingly, the midpoint redox potential values for the respective low-potential haem groups of the purified A- and B-paralogs were both clearly lower than 60 mV at pH 7.2. In addition, our data are in agreement with the ferric-reductase activities (Fig. 3a–d, f), especially with the capability of both *A. thaliana* cytochromes to reduce Fe^{3+}-EDTA (standard redox potential = +130 mV [51]). The lower specific activities for the reduction of Fe^{3+}-citrate could be explained by its higher redox potential (+200 mV [8]). For both Fe^{3+}-chelates, the A-paralog displayed a higher activity. The reduction activity of the DEPC-treated A-paralog is approximately in the same range as the unmodified B-paralog. Alternating energetically "uphill" and "downhill" electron transfer along chains of prosthetic groups is well established to occur based on work on other electron transfer proteins, such as photosynthetic reaction centres, hydrogenase [52] and dihaem-containing fumarate reductase [53], as long as the "edge-to-edge" distance between consecutive cofactors is maximally 14 Å [52] and the overall process is energetically favourable.

Finally our results indicated that the high potential haem groups of both paralogs are involved in Fe^{3+}-chelates reduction. In the tonoplast of *A. thaliana*, a vacuolar membrane transporter VIT [54] was identified. This transporter, as with all iron transporters currently known, can catalyse the transport of iron across the cell membranes only when iron is present in the reduced state (Fe^{2+}). However, due to the high reactivity of the Fe^{2+} ion (Fenton reaction [55]), iron is normally stored in the cells in the oxidised state (Fe^{3+}) in complexes with chelators. Therefore, to transport iron inside the vacuole, the Fe^{3+}-chelator complex must be reduced to Fe^{2+} and this function could be performed by the A-paralog, in the same manner as for the duodenal cyt b_{561} [10]. Since the *A*cytb_{561}-A is localised in the membrane of the tonoplast [19], the internal pH of the vacuole is 5.5 [56] and in Fig. 4 it is shown that at this pH the A-paralog is almost reducible by ascorbate, it can be speculated that if the low-potential haem of the A-paralog faces the internal side of the vacuole, its reduction by ascorbate can still occur. However ascorbate concentration into the vacuole seems to be very low and might limit the capacity of CYBASC proteins to reduce cytosolic iron chelates. In the cytosol, ascorbate is in the millimolar range or more. NRAMP3 and 4-iron transporters are specific for the Fe^{2+} transport outside the vacuole [57]. So it could be also possible that CYBASC proteins assist vacuolar iron efflux, rather than influx.

4.3. Inhibition of the low-potential haem by DEPC

DEPC can modify with high affinity histidine residues by reacting with a deprotonated nitrogen atom of the imidazole ring [58]. It has been proposed that DEPC inhibition of CYBASC proteins is caused by covalent modification of one or more of the His residues that coordinate the haem centres [46–49]. Incubation of the purified A- and B-paralogs with DEPC resulted in the inhibition of their ascorbate-dependent reduction (Table 3). One remarkable point was that after incubation with DEPC both *Arabidopsis* paralogs retained their haem groups. As the absorbance at 415 nm of the oxidised cytochromes was not affected profoundly by incubation with DEPC, inhibition by DEPC is not caused by the loss of any haem centre.

To investigate the reason(s) for this inhibition, haem redox titrations of the DEPC-modified A- and B-paralogs were performed. The redox titration of the DEPC-modified A-paralog showed clearly that the midpoint potential of the low-potential haem was modified (Supplementary Fig. S8). While the difference $\Delta E_{M,bH}$ in the midpoint potential values for the high potential haem between unmodified and DEPC-modified samples was only 47 mV, the corresponding difference is approximately five times larger for the low potential haem, $\Delta E_{M,bL}$ being 229 mV.

We could not observe this differential effect for the B-paralog: Here we found that both haem midpoint potentials were modified with $\Delta E_{M,bL} = 211$ mV and $\Delta E_{M,bH} = 186$ mV. Comparison of the amino acid sequences of A and B-paralog (Supplementary Fig. S1) reveals the presence in the B-paralog of an additional His residue in the proximity of the haem proposed to be involved in electron donation to the MDHA (His 46). This could explain why both midpoint potentials were modified in the B-paralog and not in the A-paralog.

In contrast, after incubation with DEPC and ascorbate, we found that both haem centres exhibited almost unaltered midpoint potentials compared to the unmodified samples (Table 3, Fig. 2a and b) with $\Delta E_{M,bL} = 35$ mV and $\Delta E_{M,bH} = 33$ mV for the A-paralog (Fig. S8c) and $\Delta E_{M,bL} = 21$ mV and $\Delta E_{M,bH} = 7$ mV for the B-paralog (Fig. S8f). Based on these results, we can deduce the ascorbate-binding site to be near to the low-potential haem in the A-paralog. By binding to the enzyme, ascorbate could protect the low-potential haem centre from modification by DEPC, as has been shown previously for the bovine enzyme [3,43]. The topology model, where the haem b_L centre is next to the ascorbate binding site [23,39,40,43] is in conflict with the results from Desmet et al., 2011 [20] and Liu et al., 2011 [59]. EPR measurements [20], redox- and ascorbate titrations of the wild type and variants of the cyt b_{561} proteins [20,59] were performed which indicated haem b_H to be closer to the ascorbate binding site. However, our redox titration of the different modified samples indicated the ascorbate binding to be closer to haem b_L.

Neither paralogs could be reduced fully by ascorbate (Table 3; 8% for the A-paralog and 36% for the B-paralog) and the RCA is only 11% (A-paralog) and 13% (B-paralog) after incubation with DEPC (in the absence of ascorbate). These results are generally consistent with the modified midpoint potentials. Based on the $E_{M7.2}$ values the expectation after incubation with DEPC in the presence of ascorbate would be that the haem reducibility by ascorbate is in the same range as in the control. However, we found also a significant inhibition of ascorbate oxidation activity after incubation with DEPC and ascorbate for both paralogs (42% for the A and 54% for the B-paralog) and the RCA are only 10% (A-paralog, Fig. 2c, sample

"D + A") and 3% (B-paralog, Fig. 2d, sample "D + A"). Clearly, this must be due to an additional mechanism of inhibition, unrelated to the haem E_M values [43]. In 2009, Nakanishi et al. [60,61] showed that DEPC in Zmb_{561} modified not only the histidines but also the conserved lysine 83 (corresponding to *A*cytb_{561}-A K80 and *A*cytb_{561}-B K81). This lysine 83 should be involved in the electron/proton transfer [60,61] across the membrane and/or a very important role for the ascorbate access. While the histidine residues are protected by the ascorbate between the incubation with DEPC plus ascorbate, this conserved lysine is expected to be modified by DEPC. This modification could have a significant effect on the accessibility and/or affinity of the binding site for ascorbate. This could be a possible explanation for the diminished haem reducibility and the low RCA in both paralogs.

5. Conclusion

For the first time, two CYBASC members (*A*Cytb_{561}- A and *A*Cytb_{561}- B) from *A. thaliana* have been produced both in the *E. coli* and in the *P. pastoris* expression systems. We demonstrated that the reduction of the purified paralogs by the physiological electron donor ascorbate depends on the pH. In addition we have determined specific activities of the oxidation of ascorbate and of the reduction of ferric chelates for both paralogs. Furthermore our results have confirmed an inhibition of ascorbate reduction by DEPC of both paralogs which is partially blocked by the pre-incubation with ascorbate. The $E_{M7.2}$ values of the DEPC-modified samples differed clearly from the control while our samples treated with DEPC and ascorbate displayed nearly the same E_M values as the control. In both paralogs, the haem b_L potentials are lowered by treatment with DEPC. The protection of the haem b_L potential by ascorbate indicated that the ascorbate binding site is next to the haem b_L centre. In contrast to the E_M values, the relative catalytic activities of ascorbate oxidation of both paralogs, modified with DEPC either in the presence or absence of ascorbate, were reduced to only about 10% of the control. Consequently, there must be an alternative site modified by DEPC that is not protected by ascorbate but involved in the accessibility and/or affinity of the binding site for ascorbate. The production and the characterisation presented here provide prerequisites for future structural and mechanistic analysis of members of the CYBASC protein family.

Acknowledgement

MB is supported by the DFG Research Training Group GRK845 on *Molecular, physiological and pharmacological analysis of cellular membrane transport*, TVMS was supported by a grant from the German Federal Ministry of Education, Science, Research and Technology framework programme ('BMBF-Verbundprojekt') on the *Proteome-wide Analysis of Membrane Proteins* (ProAMP). We thank Prof. Hartmut Michel for his support of the work at the MPI of Biophysics. We gratefully acknowledge Dr. Rajsekhar Paul, Hans Werner Müller and Dr. Georg Wille for kind help with the spectroelectrochemical setup. MB would like to thank Markus Höhnen (ADDITIVE GmbH) for the introduction to the software Origin 8.1G and 8.5 and Dr. Yvonne Carius for the introduction to the *Pichia pastoris* system. We thank the Deutsche Forschungsgemeinschaft (DFG), Cluster of Excellence Frankfurt (CEF) "Macromolecular Complexes", the Max Planck Society and Saarland University for funding.

Appendix A. Supplementary data

Supplementary data to this article can be found online at doi:10.1016/j.bbamem.2011.10.030.

References

[1] M. Tsubaki, F. Takeuchi, N. Nakanishi, Cytochrome b561 protein family: expanding roles and versatile transmembrane electron transfer abilities as predicted by a new classification system and protein sequence motif analyses, Biochim. Biophys. Acta 1753 (2005) 174–190.
[2] T. Flatmark, M. Gronberg, Cytochrome b561 of the bovine adrenal chromaffin granules. Molecular weight and hydrodynamic properties in micellar solutions of triton X-100, Biochem. Biophys. Res. Commun. 99 (1981) 292–301.
[3] T. Flatmark, O. Terland, Cytochrome b561 of the bovine adrenal chromaffin granules. A high potential b-type cytochrome, Biochim. Biophys. Acta 253 (1971) 487–491.
[4] D. Njus, The chromaffin vesicle and the energetics of storage organelles, J. Auton. Nerv. Syst. 7 (1983) 35–40.
[5] D. Njus, J. Knoth, C. Cook, P.M. Kelly, Electron transfer across the chromaffin granule membrane, J. Biol. Chem. 258 (1983) 27–30.
[6] D. Njus, G.K. Radda, Bioenergetic processes in chromaffin granules a new perspective on some old problems, Biochim. Biophys. Acta 463 (1978) 219–244.
[7] D. Su, J.M. May, M.J. Koury, H. Asard, Human erythrocyte membranes contain a cytochrome b561 that may be involved in extracellular ascorbate recycling, J. Biol. Chem. 281 (2006) 39852–39859.
[8] A. Berczi, D. Su, H. Asard, An Arabidopsis cytochrome b561 with trans-membrane ferrireductase capability, FEBS Lett. 581 (2007) 1505–1508.
[9] S. Ludwiczek, F.I. Rosell, M.L. Ludwiczek, A.G. Mauk, Recombinant expression and initial characterization of the putative human enteric ferric reductase Dcytb, Biochemistry 47 (2008) 753–761.
[10] A.T. McKie, D. Barrow, G.O. Latunde-Dada, A. Rolfs, G. Sager, E. Mudaly, M. Mudaly, C. Richardson, D. Barlow, A. Bomford, T.J. Peters, K.B. Raja, S. Shirali, M.A. Hediger, F. Farzaneh, R.J. Simpson, An iron-regulated ferric reductase associated with the absorption of dietary iron, Science 291 (2001) 1755–1759.
[11] J.S. Oakhill, S.J. Marritt, E.G. Gareta, R. Cammack, A.T. McKie, Functional characterization of human duodenal cytochrome b (Cybrd1): redox properties in relation to iron and ascorbate metabolism, Biochim. Biophys. Acta 1777 (2008) 260–268.
[12] D. Su, H. Asard, Three mammalian cytochromes b561 are ascorbate-dependent ferrireductases, FEBS J. 273 (2006) 3722–3734.
[13] H. Asard, J. Kapila, W. Verelst, A. Berczi, Higher-plant plasma membrane cytochrome b561: a protein in search of a function, Protoplasma 217 (2001) 77–93.
[14] D. Bashtovyy, A. Berczi, H. Asard, T. Pali, Structure prediction for the di-heme cytochrome b561 protein family, Protoplasma 221 (2003) 31–40.
[15] C.P. Ponting, Domain homologues of dopamine beta-hydroxylase and ferric reductase: roles for iron metabolism in neurodegenerative disorders? Hum. Mol. Genet. 10 (2001) 1853–1858.
[16] S. Scagliarini, L. Rotino, I. Bäurle, H. Asard, P. Pupillo, P. Trost, Initial purification study of the cytochrome b561 of bean hypocotyl plasma membrane, Protoplasma 205 (1998) 66–73.
[17] P. Trost, A. Berczi, F. Sparla, G. Sponza, B. Marzadori, H. Asard, P. Pupillo, Purification of cytochrome b561 from bean hypocotyls plasma membrane. Evidence for the presence of two heme centers, Biochim. Biophys. Acta 1468 (2000) 1–5.
[18] V. Preger, N. Tango, C. Marchand, S.D. Lemaire, D. Carbonera, M. Di Valentin, A. Costa, P. Pupillo, P. Trost, Auxin-responsive genes *AIR12* code for a new family of plasma membrane *b*-type cytochromes specific to flowering plants, Plant Physiol. 150 (2009) 606–620.
[19] D. Griesen, D. Su, A. Berczi, H. Asard, Localization of an ascorbate-reducible cytochrome b561 in the plant tonoplast, Plant Physiol. 134 (2004) 726–734.
[20] F. Desmet, A. Bérczi, L. Zimányi, H. Asard, S. Van Doorslaer, Axial ligation of the high-potential heme center in an Arabidopsis cytochrome b561, FEBS Lett. 585 (2011) 545–548.
[21] Y. Nanasato, K. Akashi, A. Yokota, Co-expression of cytochrome b561 and ascorbate oxidase in leaves of wild watermelon under drought and high light conditions, Plant Cell Physiol. 46 (2005) 1515–1524.
[22] V. Preger, A. Pesaresi, P. Pupillo, P. Trost, Identification of an ascorbate-dependent cytochrome *b* of the tonoplast membrane sharing biochemical features with members of the cytochrome b_{561} family, Planta 220 (2005) 365–375.
[23] N. Nakanishi, F. Takeuchi, M. Tsubaki, Histidine cycle mechanism for the concerted proton/electron transfer from ascorbate to the cytosolic haem b centre of cytochrome b_{561}: a unique machinery for the biological transmembrane electron transfer, J. Biochem. 142 (2007) 553–560.
[24] W. Verelst, H. Asard, A phylogenetic study of cytochrome b561 proteins, Genome Biol. 4 (2003) R38.
[25] W. Verelst, H. Asard, Analysis of an *Arabidopsis thaliana* protein family, structurally related to cytochromes b561 and potentially involved in catecholamine biochemistry in plants, J. Plant Physiol. 161 (2004) 175–181.
[26] W. Verelst, J. Kapila, J. De Almeida Engler, J.M. Stone, R. Caubergs, H. Asard, Tissue-specific expression and developmental regulation of cytochrome b561 genes in *Arabidopsis thaliana* and *Raphanus sativus*, Physiol. Plant. 120 (2004) 312–318.
[27] H.M. Weiss, W. Haase, H. Michel, H. Reilander, Comparative biochemical and pharmacological characterization of the mouse 5HT5A 5-hydroxytryptamine receptor and the human beta2-adrenergic receptor produced in the methylotrophic yeast *Pichia pastoris*, Biochem. J. 330 (1998) 1137–1147.
[28] B. Singer, L. Sun, H. Fraenkel-Conrat, Effects of alkylation of phosphodiesters and of bases of infectivity and stability of tobacco mosaic virus RNA, Proc. Natl. Acad. Sci. U. S. A. 72 (1975) 2232–2236.
[29] S. Surade, M. Klein, P.C. Stolt-Bergner, C. Muenke, A. Roy, H. Michel, Comparative analysis and "expression space" coverage of the production of prokaryotic membrane proteins for structural genomics, Protein Sci. 15 (2006) 2178–2189.

[30] P.K. Smith, R.I. Krohn, G.T. Hermanson, A.K. Mallia, F.H. Gartner, M.D. Provenzano, E.K. Fujimoto, N.M. Goeke, B.J. Olson, D.C. Klenk, Measurement of protein using bicinchoninic acid, Anal. Biochem. 150 (1985) 76–85.
[31] W. Liu, Y. Kamensky, R. Kakkar, E. Foley, R.J. Kulmacz, G. Palmer, Purification and characterization of bovine adrenal cytochrome b561 expressed in insect and yeast cell systems, Protein Expr. Purif. 40 (2005) 429–439.
[32] D. Moss, E. Nabedryk, J. Breton, W. Mantele, Redox-linked conformational changes in proteins detected by a combination of infrared spectroscopy and protein electrochemistry, Eur. J. Biochem. 187 (1990) 565–572.
[33] C.R.D. Lancaster, R. Gross, A. Haas, M. Ritter, W. Mäntele, J. Simon, A. Kröger, Essential role of Glu-C66 for menaquinol oxidation indicates transmembrane electrochemical potential generation by Wolinella succinogenes fumarate reductase, Proc. Natl. Acad. Sci. U. S. A. 97 (2000) 13051–13056.
[34] C.R.D. Lancaster, U.S. Sauer, R. Gross, A.H. Haas, J. Graf, H. Schwalbe, W. Mäntele, J. Simon, M.G. Madej, Experimental support for the “E-pathway hypothesis” of coupled transmembrane e- and H+ transfer in dihemic quinol:fumarate reductase, Proc. Natl. Acad. Sci. U. S. A. 102 (2005) 18860–18865.
[35] M. Mileni, A.H. Haas, W. Mäntele, J. Simon, C.R.D. Lancaster, Probing heme propionate involvement in transmembrane proton transfer coupled to electron transfer in dihemic quinol:fumarate reductase by ^{13}C-labeling and FTIR difference spectroscopy, Biochemistry 44 (2005) 16718–16728.
[36] K. Kobayashi, M. Tsubaki, S. Tagawa, Distinct roles of two heme centers for transmembrane electron transfer in cytochrome b561 from bovine adrenal chromaffin vesicles as revealed by pulse radiolysis, J. Biol. Chem. 273 (1998) 16038–16042.
[37] M. Tsubaki, M. Nakayama, E. Okuyama, Y. Ichikawa, H. Hori, Existence of two heme B centers in cytochrome b561 from bovine adrenal chromaffin vesicles as revealed by a new purification procedure and EPR spectroscopy, J. Biol. Chem. 272 (1997) 23206–23210.
[38] W. Liu, C.E. Rogge, Y. Kamensky, A.L. Tsai, R.J. Kulmacz, Development of a bacterial system for high yield expression of fully functional adrenal cytochrome b561, Protein Expr. Purif. 56 (2007) 145–152.
[39] A. Berczi, D. Su, M. Lakshminarasimhan, A. Vargas, H. Asard, Heterologous expression and site-directed mutagenesis of an ascorbate-reducible cytochrome b561, Arch. Biochem. Biophys. 443 (2005) 82–92.
[40] F. Takeuchi, H. Hori, E. Obayashi, Y. Shiro, M. Tsubaki, Properties of two distinct heme centers of cytochrome b561 from bovine chromaffin vesicles studied by EPR, resonance Raman, and ascorbate reduction assay, J. Biochem. 135 (2004) 53–64.
[41] D.K. Apps, M.D. Boisclair, F.S. Gavine, G.W. Pettigrew, Unusual redox behaviour of cytochrome b561 from bovine chromaffin granule membranes, Biochim. Biophys. Acta 764 (1984) 8–16.
[42] E. Gasteiger, C. Hoogland, A. Gattiker, S. Duvaud, M.R. Wilkins, R.D. Appel, A. Bairoch, Protein Identification and Analysis Tools on the ExPASy Server, first ed., Humana Press, 2005, pp. 571–607.
[43] T. Takigami, F. Takeuchi, M. Nakagawa, T. Hase, M. Tsubaki, Stopped-flow analyses on the reaction of ascorbate with cytochrome b561 purified from bovine chromaffin vesicle membranes, Biochemistry 42 (2003) 8110–8118.
[44] S. Wanduragala, D.S. Wimalasena, D.C. Haines, P.K. Kahol, K. Wimalasena, pH-induced alteration and oxidative destruction of heme in purified chromaffin granule cytochrome b(561): implications for the oxidative stress in catecholaminergic neurons, Biochemistry 42 (2003) 3617–3626.
[45] E. Okuyama, R. Yamamoto, Y. Ichikawa, M. Tsubaki, Structural basis for the electron transfer across the chromaffin vesicle membranes catalyzed by cytochrome b561: analyses of cDNA nucleotide sequences and visible absorption spectra, Biochim. Biophys. Acta 1383 (1998) 269–278.
[46] B.H. Kipp, P.M. Kelley, D. Njus, Evidence for an essential histidine residue in the ascorbate-binding site of cytochrome b561, Biochemistry 40 (2001) 3931–3937.
[47] D. Njus, M. Wigle, P.M. Kelley, B.H. Kipp, H.B. Schlegel, Mechanism of ascorbic acid oxidation by cytochrome b(561), Biochemistry 40 (2001) 11905–11911.
[48] F. Takeuchi, K. Kobayashi, S. Tagawa, M. Tsubaki, Ascorbate inhibits the carbethoxylation of two histidyl and one tyrosyl residues indispensable for the transmembrane electron transfer reaction of cytochrome b561, Biochemistry 40 (2001) 4067–4076.
[49] M. Tsubaki, K. Kobayashi, T. Ichise, F. Takeuchi, S. Tagawa, Diethyl pyrocarbonate modification abolishes fast electron accepting ability of cytochrome b561 from ascorbate but does not influence electron donation to monodehydroascorbate radical: identification of the modification sites by mass spectrometric analysis, Biochemistry 39 (2000) 3276–3284.
[50] D.L. Zhang, D. Su, A. Berczi, A. Vargas, H. Asard, An ascorbate-reducible cytochrome b561 is localized in macrophage lysosomes, Biochim. Biophys. Acta 1760 (2006) 1903–1913.
[51] M.J. Holden, D.G. Luster, R.L. Chaney, T.J. Buckhout, C. Robinson, Fe-chelate reductase activity of plasma membranes isolated from tomato (*Lycopersicon esculentum* Mill.) roots: comparison of enzymes from Fe-deficient and Fe-sufficient roots, Plant Physiol. 97 (1991) 537–544.
[52] C.C. Page, C.C. Moser, X. Chen, P.L. Dutton, Natural engineering principles of electron tunnelling in biological oxidation–reduction, Nature 402 (1999) 47–52.
[53] M.G. Madej, H.R. Nasiri, N.S. Hilgendorff, H. Schwalbe, C.R.D. Lancaster, Evidence for transmembrane proton transfer in a dihaem-containing membrane protein complex, EMBO J. 25 (2006) 4963–4970.
[54] S.A. Kim, T. Punshon, A. Lanzirotti, L. Li, J.M. Alonso, J.R. Ecker, J. Kaplan, M.L. Guerinot, Localization of iron in Arabidopsis seed requires the vacuolar membrane transporter VIT1, Science 314 (2006) 1295–1298.
[55] M.J. Burkitt, Chemical, biological and medical controversies surrounding the Fenton reaction, Prog. React. Kinet. Mech. 28 (2003) 75–104.
[56] Y. Mathieu, J. Guern, A. Kurkdjian, P. Manigault, J. Manigault, T. Zielinska, B. Gillet, J.C. Beloei, J.Y. Lallemand, Regulation of vacuolar pH of plant cells: I. isolation and properties of vacuoles suitable for P NMR studies, Plant Physiol. 89 (1989) 19–26.
[57] J. Morrissey, M.L. Guerinot, Iron uptake and transport in plants: the good, the bad, and the ionome, Chem. Rev. 109 (2009) 4553–4567.
[58] E.W. Miles, Modification of histidyl residues in proteins by diethylpyrocarbonate, Methods Enzymol. 47 (1977) 431–442.
[59] W. Liu, G.F.Z. da Silva, G. Wu, G. Palmer, A. Tsai, R.J. Kulmacz, Functional and structural roles of residues in the third extramembranesegment (EM3) of adrenal cytochrome b561, Biochemistry 15 (2011) 3149–3160.
[60] N. Nakanishi, M.M. Rahman, Y. Sakamoto, M. Miura, F. Takeuchi, S.Y. Park, M. Tsubaki, Inhibition of electron acceptance from ascorbate by the specific N-carbethoxylations of Maize Cytochrome b561: a common mechanism for the transmembrane electron transfer in cytochrome b561 protein family, J. Biochem. 146 (2009) 857–866.
[61] N. Nakanishi, M.M. Rahman, Y. Sakamoto, T. Takigami, K. Kobayashi, H. Hori, T. Hase, S.Y. Yong Park, M. Tsubaki, Importance of the conserved lysine 83 residue of Zea mays cytochrome b(561) for ascorbate-specific transmembrane electron transfer as revealed by site-directed mutagenesis studies, Biochemistry 48 (2009) 10665–10678.
[62] H. Ohno, J. Blackwell, A.M. Jamieson, D.A. Carrino, A.I. Caplan, Calibration of the relative molecular mass of proteoglycan subunit by column chromatography on Sepharose CL-2B, Biochem. J. 235 (1986) 553–557.